A 570-kbps ASK Demodulator Without External Capacitors for Low-Frequency Wireless Bio-Implants

Chua-Chin Wang [*,a], Tzung-Je Lee [a], U Fat Chio [b], Yu-Tzu Hsiao [c] Jia-Jin J. Chen [d]

[a] *Department of Electrical Engineering, National Sun Yat-Sen University, Kaohsiung, 80424 Taiwan.*

[b] *DenMOS Technology Inc., Hsinchu, Taiwan.*

[c] *UCA Technology Inc., Taiwan.*

[d] *Institute of Biomedical Engineering, National Cheng Kung University, Taiwan.*

Abstract

This paper proposes a novel structure of ASK demodulators, which requires no external capacitors, for implantable micro-stimulators. By using a traditional β multiplier reference to detect the signal envelope, followed by a Schmitt trigger and a load driver, the large off-chip capacitor in traditional ASK demodulators is not required any more. Therefore, the proposed circuit possesses small area to be integrated in an SOC chip. Besides, due to the lack of the large capacitor, the proposed circuit can operate with a higher data rate using lower frequency carriers. The proposed circuit is integrated in an implantable micro-stimulator on silicon using 0.35 μm 2P4M CMOS process. The area of the proposed circuit occupies merely 0.039 mm^2 with a maximum power dissipation of less than 12 mW (including the power consumption of the analog circuits of the micro-stimulator) by measurement results on silicon. Moreover, the measurement results verify that the proposed ASK demodulator can detect the ASK modulated signal up to 570 kbps data rate at 2 MHz carrier frequency when the modulation index is 10%.

Key words: ASK, bio-implant, micro-stimulator, data rate, modulation index

* The corresponding author.

Email addresses: ccwang@ee.nsysu.edu.tw (Chua-Chin Wang), waller@vlsi.ee.nsysu.edu.tw (Tzung-Je Lee), alpha_chio@mail.denmos.com.tw (U Fat Chio), ythsiao@uca.com.tw (Yu-Tzu Hsiao), jason@jason.bme.ncku.edu.tw (Jia-Jin J. Chen).

1 Introduction

The implantable micro-stimulator is one of the recent major medical research topics. It is widely used in bladder leakage control [1], muscle nerve stimulation [2], and cochlear implants [3]. The implanted device can be powered by a RF transcutaneous magnetic coupling method using an external transmitter coil to power and communicate with the implanted devices. One of the most important issues for implantable devices is the size. Notably, living tissues have a high absorption rate if the frequency of the wireless RF induction is high, which will cause the temperature of the living tissues to rise drastically. Therefore, all of the RF coupling methods used for biomedical implants are really low, e.g., 13.56 MHz, or even 2 MHz. Meanwhile, most of the prior implanted devices adopted ASK (amplitude shift keying) modulation because of the simplicity of the demodulation circuit [4]. However, those prior designs contained a large capacitor to cope with the low RF frequency [5], [6], [7]. The capacitors are even larger than 10 pF. Such a large capacitor either occupies a huge area in the SOC (system-on-chip) chip or becomes a discrete component on a PCB. Either way will increase the size of the implants. Reducing the numbers of the these large components is important for integration of an SOC chip. Thus, we propose an ASK demodulator design containing no large capacitor at all such that a much smaller size can be achieved. The entire circuit is carried out using TSMC (Taiwan Semiconductor Manufacturing Company) 0.35 μm 2P4M CMOS technology. The area of the proposed ASK demodulator is 0.07215 mm^2, which is smaller than all of the prior works.

Moreover, a high carrier frequency and the higher modulation index usually imply a high data rate. However, the high carrier frequency might increase the power consumption of the overall system. Furthermore, high frequency signal could be absorbed by the tissues as we mentioned in the previous paragraph such that the transmission efficiency is decreased and the tissue might be hurt. Thus, the carrier frequency is often chosen to be less than 15 MHz for most of the implantable applications [4]. Besides, because the implantable devices usually employ wireless link to obtain the required power from an external transmitter, a small modulation index is much more preferred to improve the stability of the received power when the ASK modulation is used. Thus, it is preferred that high data rate can be achieved at such a low modulation index and a low carrier frequency for the bio-implant. The measurement results reveal that a 570 kbps data rate can be accomplished by the proposed ASK demodulator for 10% modulation index at 2 MHz carrier frequency. The physical measurements of the prototype chip justify the outstanding performance of the proposed design.

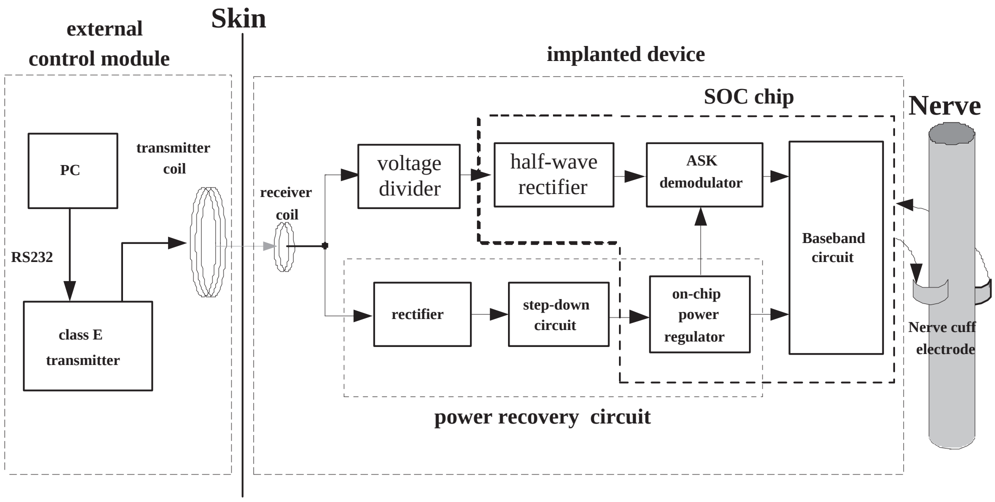

Fig. 1. Wireless neural stimulating system.

2 ASK Demodulator without External Capacitors

The entire micro-stimulator system is given in Fig. 1. The external control module includes a PC, a class E amplifier and a transmitter coil. Amplitude shift keying (ASK) modulation protocol is employed to transfer the external control data and power to the internal stimulation chip by the class E amplifier. An on-chip power regulator is required to supply a stable VDD output voltage to the internal core by regulating the power generated by the on-board coupling coil. The baseband circuit decodes the command from the ASK demodulator and executes the corresponding stimulation. The proposed ASK demodulator which employs no external capacitors is carried out in such a typical implantable micro-stimulator.

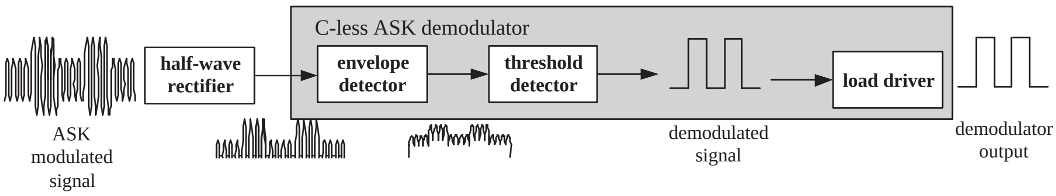

Fig. 2. The data extraction process of the ASK modulated signal.

2.1 Structure of the proposed ASK demodulator

The data extraction process for the proposed ASK modulated signal is shown in Fig. 2, where the half-wave rectifier can be implemented by a unity gain buffer using a two-stage operational amplifier for clamping the positive voltage. It could avoid the large-area penalty provided that a diode is used as the rectifier. The proposed ASK demodulator includes three parts : an envelope detector, a threshold detector, and a load driver, as shown in Fig. 3. Notably, VDD_OUT is a 3.3 V power supply voltage supplied by the on-chip power regulator.

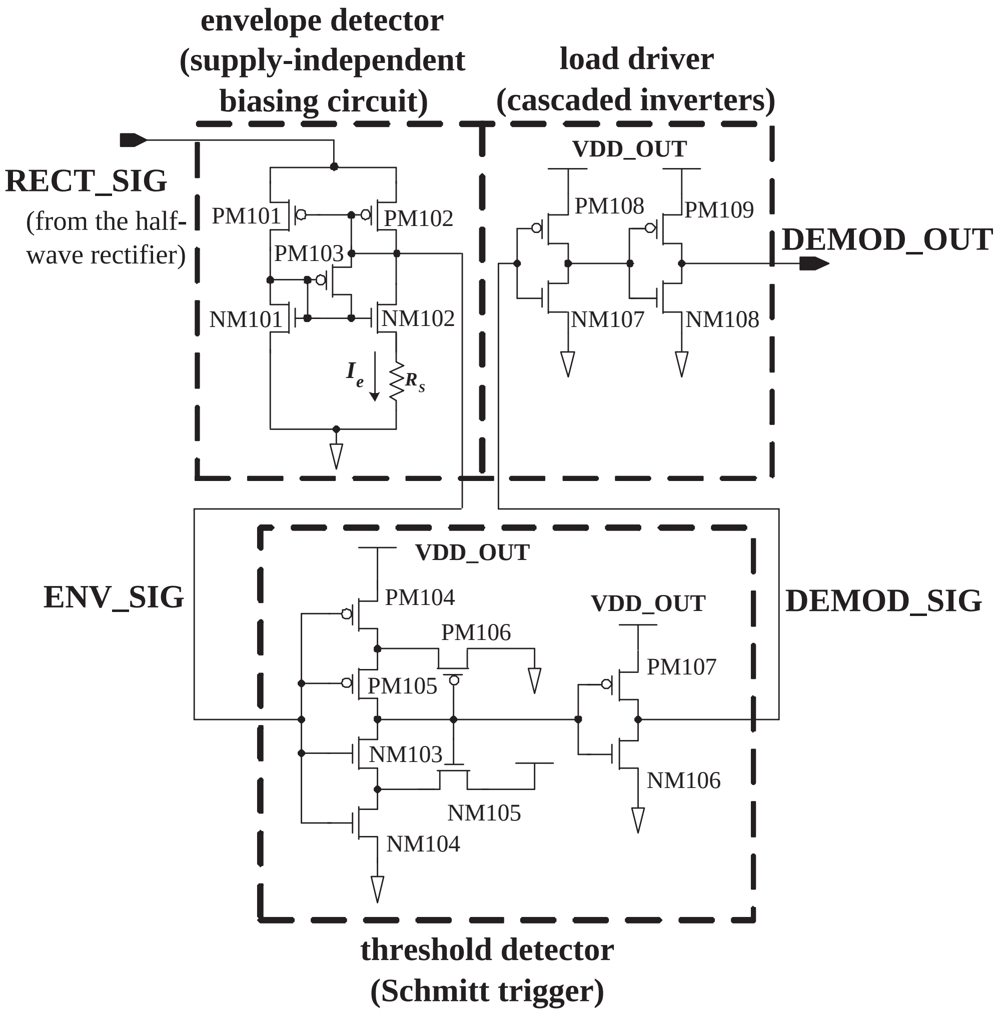

Fig. 3. Schematic of the proposed ASK demodulator.

Envelope detector: The proposed ASK demodulator employs a tradition supply-independent current bias, which is known as the β multiplier reference, to perform the envelope detection. Notably, the node to supply voltage in the traditional β multiplier reference is the input of the envelope detector in this work. Intuitively, because the current through PM102, I_e, is ideally independent to the rectified signal, RECT_SIG, at low frequency, the voltage drop on PM102, V_{GS_PM102}, might be constant regardless of the variation of RECT_SIG. Thus, the envelope output, ENV_SIG, depends on the the variation of RECT_SIG. Therefore, the supply-independent current bias circuit can trace the envelope of the half-wave rectifier's output.

According to [8], if we ignore the body effect, the supply-independent current can be expressed by

$$I_e = K_1 \cdot \frac{1}{K_n'(W/L)_{NM101}R_s^2}, \tag{1}$$

where $K_n' = \mu_n C_{ox}$, μ_n is the electron mobility, C_{ox} is the gate oxide capacitance per unit area, $K_1 = \frac{2(\sqrt{K}-1)^2}{K}$, and K is the ratio of the aspect ratio of NM101 to that of NM102.

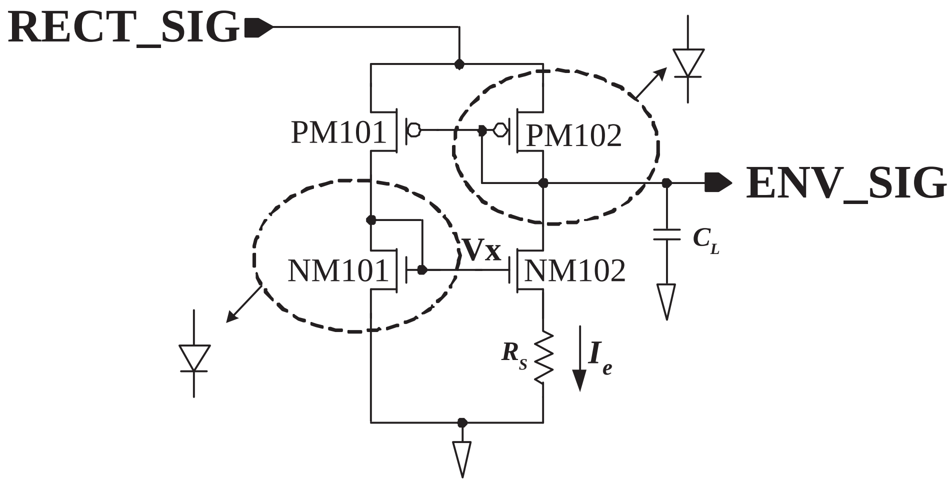

Fig. 4. The equivalent circuit of the envelope detector.

The input of the envelope detector is a DC voltage coupling with a large ripple. Because PM103 is a start-up transistor, it can be ignored when the circuit normally operates. The equivalent circuit of the envelope detector is shown in Fig. 4. The transistor NM101 is diode-connected such that the voltage Vx is a DC voltage approximately equal to the threshold voltage of NM101. By the parasitic LPF (low-pass filter) constructed by the channel resistor of PM101 and the gate capacitor of NM102, a quite small ripple is coupled on Vx. Thus, Vx determines the operating point of the proposed envelope detector. This implies that PM101, PM102, NM101 and NM102 operates in saturation region. Therefore, the current through PM102 can be expressed to be

$$I_e = \frac{1}{2} \cdot K_p' \cdot (\frac{W}{L})_{PM102} \cdot (V_{GS\_PM102} - V_{THP})^2, \tag{2}$$

where $K_p' = \mu_p C_{ox}$, and μ_p is the hole mobility of PMOS.

The output of the envelope detector can be expressed by ENV_SIG=RECT_SIG-V_{GS_PM102}. By resolving Eqn. (1) and (2), V_{GS_PM102} can be obtained. Thus, ENV_SIG is found to be

$$\mathrm{ENV\_SIG} = \mathrm{RECT\_OUT} - V_{THP} - B \cdot \sqrt{\frac{1}{R_s^2 K_n' K_p'}} \tag{3}$$

$$B = \sqrt{\frac{2 \cdot K_1}{(W/L)_{NM101}(W/L)_{PM102}}}$$

After taking the partial derivative of ENV_SIG to RECT_OUT, we have

$$\frac{\partial \mathrm{ENV\_SIG}}{\partial \mathrm{RECT\_OUT}} = 1 \tag{4}$$

Eqn. (3) reveals that the DC voltage of ENV_SIG would be a voltage drop from the DC voltage of REC_SIG. Eqn. (4) indicates that the variation of the DC voltage of ENV_SIG and REC_SIG are the same. Since the amplitude of ASK modulated signal for logic 1 is larger than that for logic 0, the DC level of REC_OUT would be at a higher voltage for logic 1 than that for logic 0. Besides, the carrier components need to be removed. The MOS resistor $(gm_{PM102})^{-1}$ and the loading capacitor C_L behave as a low-pass filter. Moreover, the channel resistors of PM102 and NM102 and the resistor R_S become a string of resistors. With the effect of the low-pass filter and the resistor string, the carrier components at ENV_SIG is suppressed. Therefore, the DC level of ENV_SIG is very close to the envelope of the rectified signal.

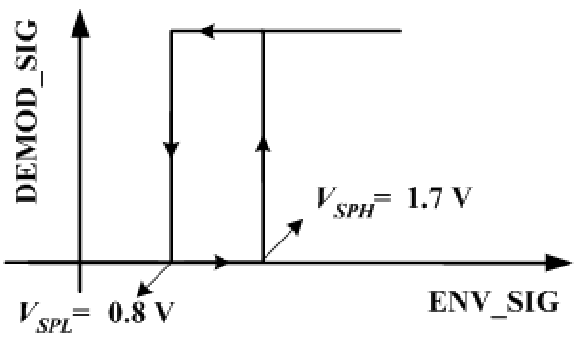

Fig. 5. Transfer characteristic curve of the Schmitt trigger.

Threshold detector: Because ENV_SIG is coupled with a ripple from 0.95 V to 2.02 V for an encoded "1" and from 0.36 V to 1.02 V for an encoded "0," the raw digital data signal generated by the envelope detector needs to be sliced by a Schmitt trigger circuit to attain a full-swing logical output. Fig. 5 is the transfer curve of the Schmitt trigger. The low switching voltage, V_{SPL}, and the high switching voltage, V_{SPH}, are chosen to be 0.8 V and 1.7 V, respectively, according to Eqn. (5) and (6) [9].

$$\frac{\mathrm{VDD\_OUT} - V_{SPH}}{V_{SPH} - V_{THN}} = \sqrt{\frac{\beta_{NM104}}{\beta_{NM105}}} = K_2 \tag{5}$$

$$\frac{V_{SPL}}{\text{VDD\_OUT} - V_{SPL} - V_{THP}} = \sqrt{\frac{\beta_{PM104}}{\beta_{PM106}}} = K_3 \tag{6}$$

Notably, the switching voltages of the Schmitt trigger depend on the output of the on-chip regulator, VDD_OUT, as shown in Eqn. (7) and (8). Moreover, the variation of the switching voltages might cause an error of the threshold detection. Therefore, the dependence of the switching voltages to VDD_OUT should be considered by the following equations to ensure the correct function.

$$\frac{\partial V_{SPH}}{\partial \text{VDD\_OUT}} = \frac{1}{1 + K_2} \tag{7}$$

$$\frac{\partial V_{SPL}}{\partial \text{VDD\_OUT}} = \frac{K_3}{1 + K_3} \tag{8}$$

Load driver: It is a buffer composed of two cascaded inverters to increase the signal driving capability.

In order to detect the ASK modulated signal correctly, the envelope signal ENV_SIG and the switching voltages (V_{SPH} and V_{SPL}) of the threshold detector should be designed by considering the variation of VDD_OUT according to Eqn. (3) $\sim$ (8). Thus, tuning the aspects (width-to-length ratio) of the transistors is very important.

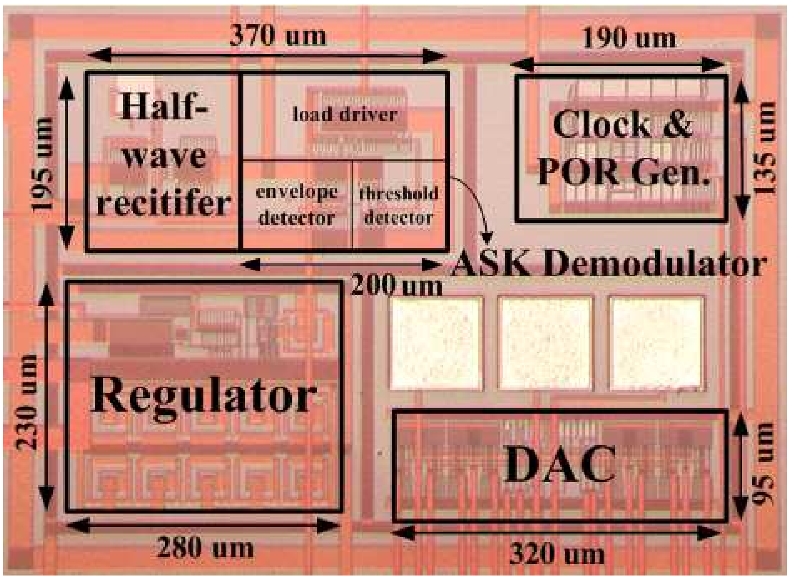

Fig. 6. The die photo of the analog circuit of the SOC chip.

3 Simulation and Measurement

The chip is designed by using TSMC (Taiwan Semiconductor Manufacturing Company) 0.35 μm 2P4M CMOS process. The die photo of the analog circuit of the implantable neural chip is shown in Fig. 6, where "Clock & POR Gen." block denotes the clock generator and the power-on-reset generator of the implantable chip. The area of the proposed ASK demodulator is 0.039 mm^2. The maximum power dissipation of the whole chip (including the circuit in Fig. 6) is measured to be less than 12 mW. Fig. 7 is the worst-case post-layout simulation given the SS (slow-slow) model, and 36^{o}C, where the ASK data extraction process shown in Fig. 2 is verified.

Fig. 8 and Fig. 9 shows the measurement results of the modulated input whose modulation index is 10% and the corresponding demodulated output given a 10 kbps and a 570 kbps data rate, respectively. Obviously, the demodulation is successful when the data rate is less than 570 kbps for 10% modulation index. Referring to Fig. 10, the glitches appear in the demodulated output if a 666 kbps data rate is supplied. However, the glitch could be removed easily by using a simple delay gate and a XOR gate. Then, the data rate higher than 570 kbps will be feasible by the proposed ASK demodulator if a de-glitch circuit is employed.

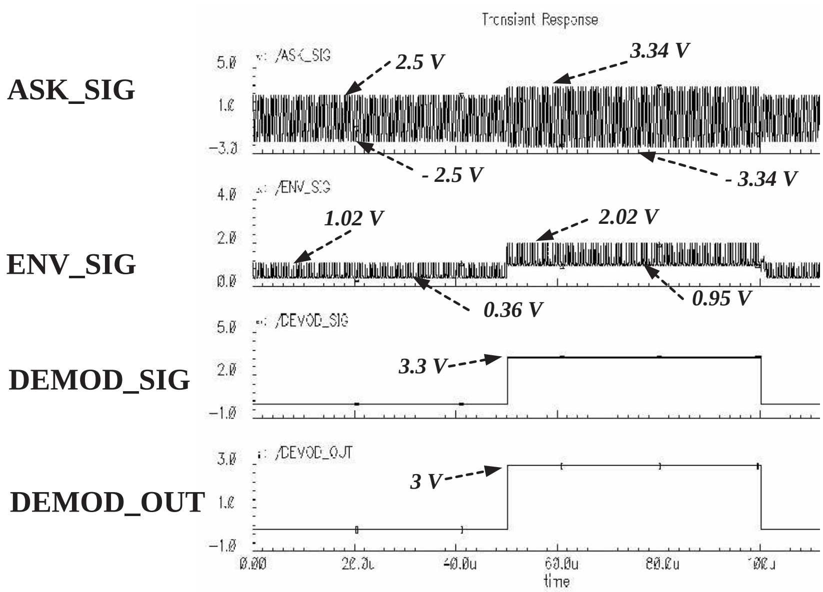

Fig. 7. Post-layout simulation result of ASK demodulator (SS, 36^{o}C).

The comparison of the proposed ASK demodulator with several prior works is summarized in Table 1. It shows that our design is the only one without using any capacitors. Notably, [4] proposed a digital ASK demodulator with a block

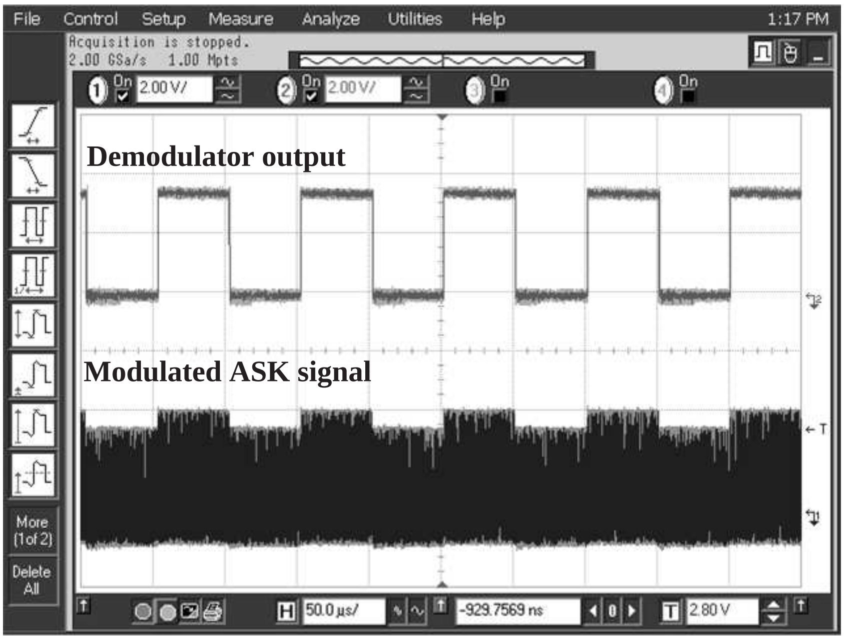

Fig. 8. Measurement result of the ASK demodulator given a 10 kbps data rate.

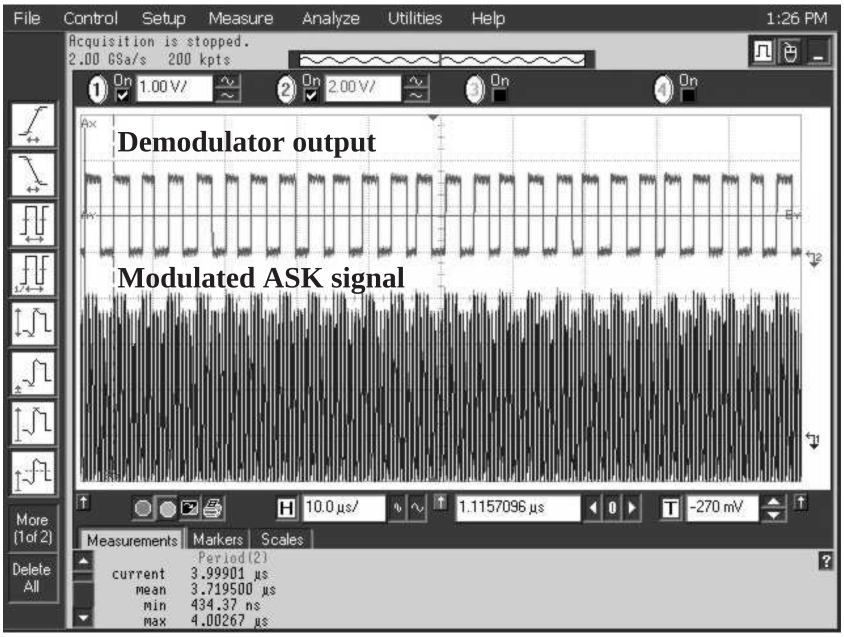

Fig. 9. Measurement result of the ASK demodulator given a 570 kbps data rate.

diagram only. The transistor number of 58 counted for the prior design [4] in Table 1 is obtained by assuming 6 for Schmitt trigger, 4 for the delay cell, 6 for the NOR gate, and 9 for the D flip-flops. Besides, the proposed ASK demodulator can accept higher data rate for a 10% modulation index (MI) than any other prior works. A figure of merit is given to compare the performance on bandwidth efficiency. FOM $= \frac{\text{data rate}}{(\text{carrier frequency})\cdot(\text{modulation index})}$. The larger FOM indicates better bandwidth efficiency. As shown by Table 1, our

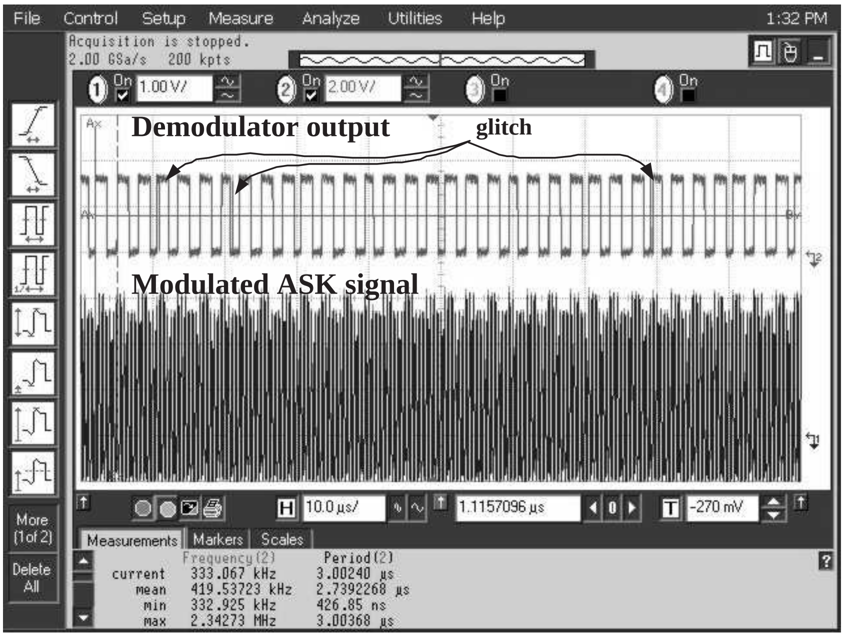

Fig. 10. Measurement result of the ASK demodulator given a 666 kbps data rate.

Table 1
Comparison with prior ASK demodulators

Design	Cap. No.	MOS No.	Area (mm^2)	Carrier (MHz)	Data Rate (kbps)	MI	FOM	Year
[4]	1	> 58	-	13.56	-	-	-	2005
[5]	1	14	0.3	10	1000	30%	3.33	2000
[7]	3	13	-	4	70	35%	0.5	2003
[10]	1	> 30	-	-	250	-	-	2004
[11]	1	19	-	10	800	100%	0.8	2000
[12]	10	> 26	0.22	10	200	10%	2	2000
[13]	3	> 43	0.18	1	18	100%	0.18	2006
[14]	1	12	-	13.56	1000	18.25%	4.04	2006
Ours	0	17	0.039	2	570	10%	28.5	2006

Note: The specifications in [14] are based on the simulation results.

design possesses a very impressive FOM compared with the rest.

4 Conclusion

A small-area solution for an implantable ASK demodulator is presented in this work. The MOS count and the capacitor size compared with prior works are clearly analyzed. The data rate for the proposed ASK demodulator is measured to be 570 kbps for a 10% modulation index at 2 MHz carrier frequency. The measurement results on silicon justify the proposed ASK demodulator.

Acknowledgment

The authors would like to express their deepest gratefulness to CIC (Chip Implementation Center) of NAPL (National Applied Research Laboratories), Taiwan, for their thoughtful chip fabrication service. Moreover, this research was partially supported by National Health Research Institutes under grant NHRI-EX95-9319EI. The authors also like to thank "Aim for Top University Plan" project of NSYSU and Ministry of Education, Taiwan, for partially supporting the research.

References

[1] J. S. Walter, J. S. Wheeler, W. Cai, W. W. King, and R. D. Wurster. Evaluation of a suture electrode for direct bladder stimulation in a lower motor neuron lesioned animal mode, IEEE Transactions on Rehabilation Engineering 7(2)(1999) 159-166.

[2] G. E. Loeb, F. J. R. Richmond, D. Olney, T. Cameron, A. C. Dupont, K. Hood, R. A. Peck, P. R. Troyk, and H. Schulman. BION^{TM}. Bionic neurons for functional and therapeutic electrical stimulation, in Proceedings of 20th IEEE Engineering in Medicine and Biology Society. vol. 5, Nov. 1998, pp. 2305-2309.

[3] R. E. Isaacs, D. J. Weber, and A. B. Schwartz. Work toward real-time control of a cortical neural prosthesis, IEEE Transactions on Rehabilation Engineering 8(2)(2000) 196-198.

[4] M. Sawan, Y. Hu, and J. Coulombe. Wireless smart implants dedicated to multichannel monitoring and microstimulation, IEEE Circuits and Systems Magazine 5(1)(2005) 21-39.

[5] W. Liu, K. Vichienchom, M. Clements, S. C. DeMarco, C. Hughes, E. McGucken, M.S. Humayun, E. De Juan, J.D. Weiland, and R. Greenberg. A neuro-stimulus chip with telemetry unit for retinal prosthetic device, IEEE Journal of Solid-State Circuits 35(10)(2000) 1487-1497.

[6] M. Barú, H. Valdenegro, C. Rossi, and F. Silveira. An ASK demodulator in CMOS technology, in Proceedings of IV Worshop de Iberchip Mar del Plata, Argentina, Mar. 1998, pp. 37-42,

[7] H. Yu, and K. Najafi. Low-power interface circuit for bio-implantable microsystems, in 2003 IEEE International Solid-States Circuits Conference. vol. 1, Feb. 2003, pp. 194-203.

[8] B. Razavi, Design of analog CMOS integrated circuits, New York: McGraw-Hill, pp. 377-380, 2001.

[9] R. J. Baker, H. W. Li, and D. E. Boyce, CMOS circuit design, layout, and simulation, 2nd Ed. New York: Wiley-Interscience, 2005.

[10] A. Djemouai, and M. Sawan. New CMOS current-mode amplitude shift keying demodulator (ASKD) dedicated for implantable electronic devices, in Proceedings of 2004 IEEE International Symposium on Circuits and Systems, ISCAS 2004, vol. 1, no. 1, May 2004, pp. 441-444.

[11] R. Harjani, O. Birkenes, and J. Kim. An IF stage design for an ASK-based wireless telemetry system, in Proceedings of 2000 IEEE International Symposium on Circuits and Systems, ISCAS 2000, vol. 1, May 2000, pp. 52-55.

[12] G. Gudnason. A low-power ASK demodulator for inductively coupled implantable electronics, in IEEE International Solid-States Circuits Conference, Sept. 2000, pp. 385-388.

[13] H. Yu, and R. Bashirullah. A Low Power ASK Clock and Data Recovery Circuit for Wireless Implantable Electronics, 2006 IEEE Custom Integrated Circuits Conference (2006) 249-252.

[14] G. B. Hmida, M. Dhieb, H. Ghariani, and M. Samet. Transcutaneous power and high data rate transmission for biomedical implants. 2006 International Conference on Design and Test of Integrated Systems in Nanoscale Technology. (2006) 374-378.